Electronic Supplementary Information

Nanosheet-to-Nanoparticle Transformation in Charged Water Microdroplets: A Pathway to Zero-Dimensional Materials†

B Krishnamurthy Spoorthi, [a] Angshuman Ray Chowdhuri,[a] Biswajit Mondal,[a] Sujan Manna,[a] Anubhav Mahapatra,[a] Amoghavarsha Ramachandra Kini [a] and Thalappil Pradeep *[ab]

[a]DST Unit of Nanoscience (DST UNS) & Thematic Unit of Excellence (TUE), Department of Chemistry, Indian Institute of Technology Madras, Chennai 600036, India.

[b]International Centre for Clean Water, 2nd Floor, B-Block, IIT Madras Research Park, Kanagam Road, Taramani, Chennai 600113, India.

Table of contents

S1. Synthesis of MoS_2 NS

Direct electrospraying of MoS_2 powder dispersions is challenging because MoS_2 is inherently hydrophobic and tends to aggregate in water due to strong van der Waals forces between its layers, leading to an unstable dispersion. To overcome this, we synthesized lower-dimensional materials, specifically the nanosheets.

To synthesize MoS_2 nanosheets (NSs), a chemical exfoliation method was applied starting from MoS_2 powder. Initially, 300 mg of MoS_2 powder was placed in a round-bottom flask under an argon atmosphere, and 3 mL of 1.6 M n-butyllithium was introduced. This mixture was stirred continuously for 48 hours under the same conditions. Afterward, the lithium-intercalated product was thoroughly washed with hexane to eliminate any residual reactants, followed by the addition of 100 mL of distilled water. The resulting mixture was then sonicated in a bath sonicator for one hour. To separate unexfoliated MoS_2, the aqueous MoS_2 NSs dispersion was centrifuged at 18,000 rpm. The quality of the synthesized MoS_2 NSs was subsequently assessed using electron microscopy and Raman spectroscopy. 500 µg of MoS_2 was then dispersed in 2 mL of water and used for the electrospray experiments.

S2. Synthesis of WS_2 nanosheet

To synthesize WS_2 nanosheets (NSs), a chemical exfoliation technique was employed starting with WS_2 powder. A total of 300 mg of WS_2 powder was placed in a round-bottom flask under an argon atmosphere, and 3 mL of 1.6 M n-butyllithium was added. The mixture was stirred continuously for 48 hours under the same conditions. Afterward, the lithium-intercalated product was repeatedly washed with hexane to remove any remaining reactants. Then, 100 mL of distilled water was added, and the product was sonicated in a bath sonicator for one hour. The resulting aqueous dispersion of WS_2 NSs was then centrifuged at 18,000 rpm to separate unexfoliated WS_2. 500 µg of WS_2 was then dispersed in 2 mL of water and used for the electrospray experiments.

S3. Synthesis of graphene oxide (GO)

Graphene oxide (GO) was synthesized from graphite powder using a modified Hummers' method. Initially, 2 g of graphite powder was oxidized in a hot solution (100°C) containing 25 mL of concentrated sulfuric acid (H_2SO_4), 4 g of potassium persulfate ($K_2S_2O_8$), and 4 g of phosphorus pentoxide (P_2O_5). The resulting dark blue mixture was allowed to cool to room temperature over 6 hours, then diluted to 200 mL with deionized water and filtered. The filtrate was dried overnight at 60°C in a hot air oven. The pre-oxidized graphite powder (2 g) was then added to 92 mL of cold H_2SO_4 (0°C) under continuous stirring in an ice bath. Potassium permanganate ($KMnO_4$, 12 g) was gradually introduced to the mixture with stirring. After 15 minutes, 2 g of sodium nitrate ($NaNO_3$) was added, and the solution was stirred for an additional 2 hours at 35°C. Distilled water (200 mL) was added dropwise during stirring. The reaction was terminated by the simultaneous addition of a mixture of 300 mL distilled water and 10 mL of 30% hydrogen peroxide (H_2O_2). The final product was sequentially washed: first with diluted hydrochloric acid (HCl, 1:10), then with water. The product was suspended in distilled water, resulting in a brown dispersion, which was dialyzed extensively to remove residual metal ions and acids. The dispersion was exfoliated via ultrasonication at 300 W for 2 hours, and unexfoliated graphite oxide was removed by centrifugation at 12,000 rpm for 20 minutes using a KUBOTA centrifuge (Tokyo, Japan).

S4. Electrospray deposition of MoS_2 NSs

For electrospray deposition, a custom-built nanoelectrospray ionization (nESI) source was utilized. This nESI source was constructed by pulling a borosilicate glass capillary (0.86 mm inner diameter and 1.5 mm outer diameter) into two segments using a micropipette puller (Sutter Instruments, USA). The tips, after pulling, were examined under an optical microscope to ensure the precision and quality of the cut. Tips with a 50 μm opening were selected for all deposition experiments.

The MoS_2 solution was loaded into the nESI tips using a micro-injector pipette tip, and a platinum (Pt) wire was inserted into the solution to act as an electrode for high-voltage application. For the electrospray deposition of MoS_2 nanosheets (NSs), an aqueous suspension of MoS_2 NSs was prepared, and the spray was directed toward a grounded substrate. The distance between the tip of the nESI source and the surface of the substrate was optimized to 5 mm.

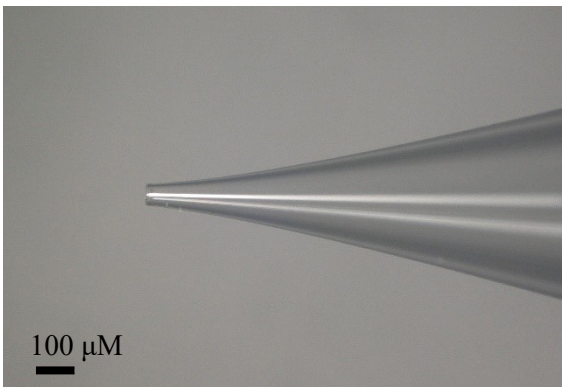

Photograph: nESI source tip used for the electrospray experiment.

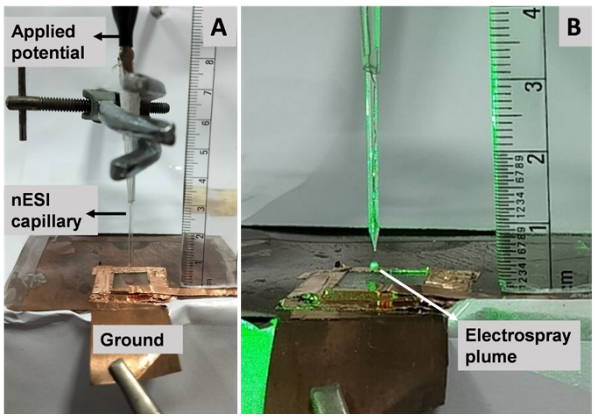

Photograph: A) nanoelectrospray set up. B) The spray plume emitted from the nanoelectrospray tip visualized by a laser torch.

For TEM analysis, 20 µL of the precursor was used. For Raman spectroscopy, 500 µL of the precursor was electrosprayed to ensure uniform and reproducible sample deposition.

Nanoparticles can be collected in larger quantities by scaling up the experiment. Increasing the dispersion volume while maintaining optimized electrospray parameters enables large-scale production, making the method suitable for catalytic applications.

S5. Electrospray deposition of WS_2 and GO NSs

Electrospray deposition of WS_2 nanosheets and graphene oxide nanosheets was carried out under similar conditions as described for MoS_2, ensuring consistency in the deposition process.

S6. The charge-induced process

In electrospray occurs due to the interaction of a high electric field with microdroplets containing dispersed nanosheets. The high electric field induces polarization within the nanosheets. This results in fragmentation of the nanosheets into nanoparticles. As the droplets shrink due to rapid solvent evaporation, Coulombic repulsion between like charges on the nanosheets further aids in breaking down the layers. Additionally, confinement effects (in tiny droplets) within the microdroplets create localized stress, promoting uniform nanoparticle formation. This dynamic interplay between electric field strength, solvent evaporation, and confinement effects ensures the reproducible synthesis of nanoparticles with controlled morphology[1].

S7. The effect of tip-collector distance on the morphology

Th optimized distance of 5 mm resulted in uniformly distributed nanoparticles. At shorter distances (<5 mm), the droplets had insufficient time for complete solvent evaporation and nanosheet fragmentation, leading to particle aggregation and partially fragmented nanosheets. Conversely, at longer distances (>5 mm), the electric field strength weakened, resulting in incomplete transformations and the formation of irregular, broken sheets. This behavior can be attributed to two primary factors:

Electric Field Dynamics: The strength of the electric field decreases with increased distance between the emitter and collector, impacting the Coulombic forces responsible for nanosheet disintegration.

Time for Solvent Evaporation: Shorter distances limit the time available for solvent evaporation, preventing complete fragmentation, whereas excessive distances lead to reduced field effects and inefficient particle formation.

S8. Plausible reasons for the effect of evaporation on observed morphology

1. Coulombic Forces and Surface Charge Effects: During the electrospray process, high electric fields induce Coulombic forces and surface charges on the MoS_2 nanosheets. These forces disrupt interlayer van der Waals interactions and create mechanical stress, facilitating nanosheet fragmentation into smaller particles.

2. Localized Confinement and Supersaturation: The rapid solvent evaporation reduces the droplet volume swiftly, leading to confinement effects. This localized confinement increases the concentration of MoS_2 nanosheets within the droplet, enhancing the likelihood of structural rearrangements due to surface energy minimization.

3. Fragmentation and Morphological Changes: The shrinking microdroplet environment, coupled with strong surface tension, promotes bending, folding, and fragmentation of the 2D nanosheets into 0D nanoparticles. The rapid evaporation also provides insufficient time for re-stacking, ensuring uniform nanoparticle formation with narrow size distributions, as confirmed by TEM and Raman spectroscopy in our study.

S9. The confinement effect

Microdroplets are tiny reaction vessels. The confinement effects are embodied in the charged microdroplet environment created during the electrospray process. These effects are discussed and supported by the following observations and findings:

1. Droplet Shrinkage and Concentration Effects: As the solvent rapidly evaporates, the droplet volume decreases, leading to spatial confinement of MoS_2 nanosheets within the microdroplet. This enhances the local concentration of nanosheets and promotes their fragmentation.

2. TEM Evidence of Morphological Transformation: Figure 1 shows the transformation of MoS_2 nanosheets into uniformly distributed nanoparticles with narrow size distributions. This uniformity arises from confinement effects that restrict random aggregation and allow controlled fragmentation.

3. Electric Field and Surface Stress: The manuscript highlights how high electric fields within the charged microdroplets create surface stress and induce structural rearrangements. These effects are amplified by the droplet's shrinking size, as described in the discussion on electrospray parameters and their influence on morphology.

4. Surface Energy Minimization: The confinement effects lead to surface energy minimization, promoting bending, folding, and fragmentation of nanosheets into stable nanoparticles, as explained in the context of TEM and Raman data.

S10. The effect of surface charge

We attribute that the surface charge is formed during the electrospray process due to the high electric field applied to the dispersion. The electrospray process generates charged microdroplets, which undergo fission due to Coulomb repulsion as the solvent evaporates and the charge density increases. From the literature, it is known that at low flow rates (typically ~5 μL min^{-1}), the resulting droplets have a narrow size distribution, with the most abundant droplet radius being ~1.5 μm. Each of these droplets carry a charge of approximately ~10^{-14} C, corresponding to ~60,000 singly charged ions[2]. This process produces smaller tiny droplets via Coulomb fission, leading to high charge densities that polarize the MoS_2 nanosheets. The Coulombic forces induced by this polarization disrupt van der Waals interactions, fragmenting the nanosheets into nanoparticles. These insights highlight the critical role of droplet charge in driving nanosheet-to-nanoparticle transformations, as observed in our study.

Evidence for surface charge: TEM Analysis shows the transformation of nanosheets into uniformly distributed nanoparticles, consistent with Coulombic fragmentation. The shifts in E_{2g}^1 and A_{1g} modes in

the Raman spectroscopy confirm the reduced interlayer coupling due to charge-induced stress. Fragmentation occurs optimally at 3.0 kV, while lower voltages result in incomplete transformation, confirming the role of surface charge.

Supplementary 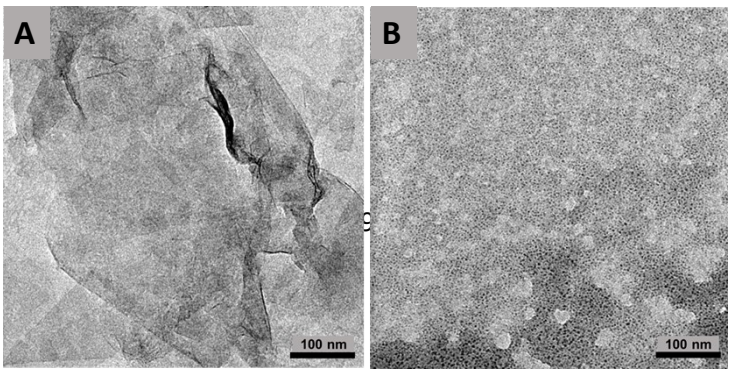

figures

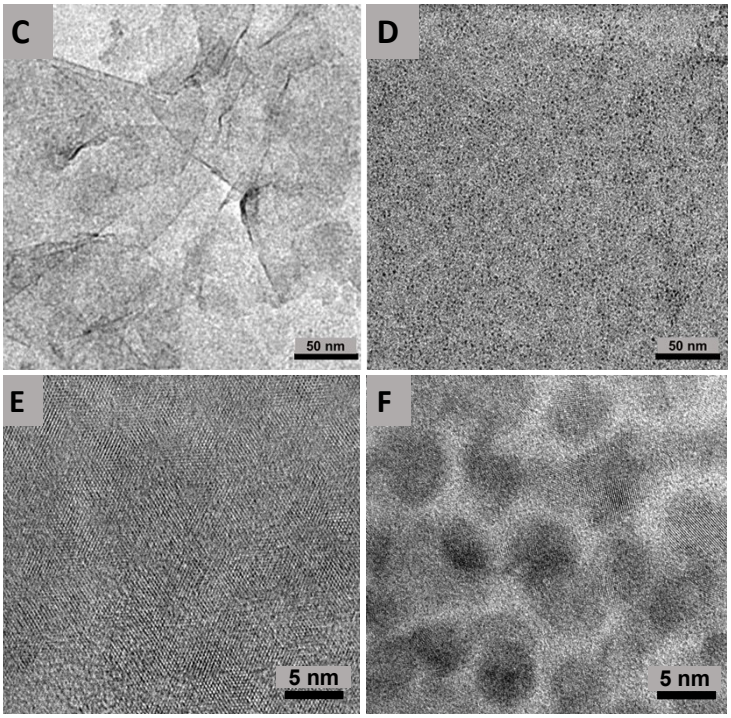

Fig. S1: Comparison of MoS_2 nanosheet before and after electrospray at different magnifications. A, C, E) As synthesised MoS_2 nanosheets before electrospray. B, D, F) MoS_2 nanoparticles formed after the electrospray.

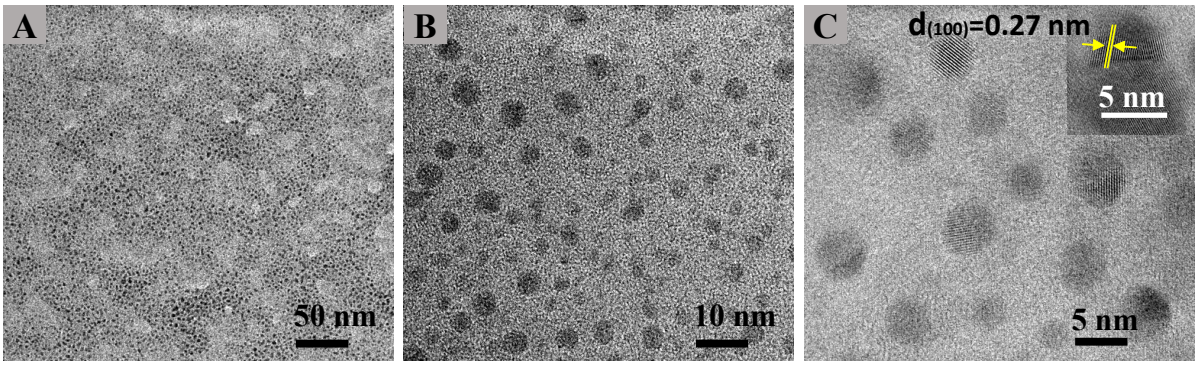

Fig. S2: TEM images showing MoS_2 nanoparticles at various magnifications. High resolution image in C shows the d spacing of (100) MoS_2.

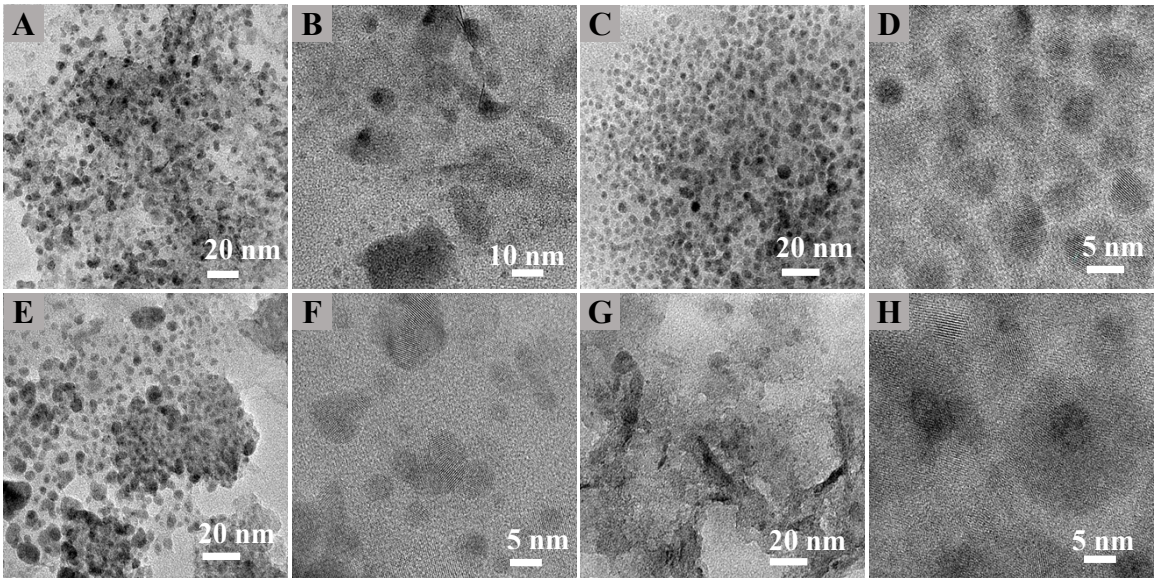

Fig. S3: Effect of distance between the emitter to the collector on the morphology of the electrosprayed MoS_2. A,B) 3 mm, C,D) 7 mm, E,F) 9 mm and G,H) 11 mm.

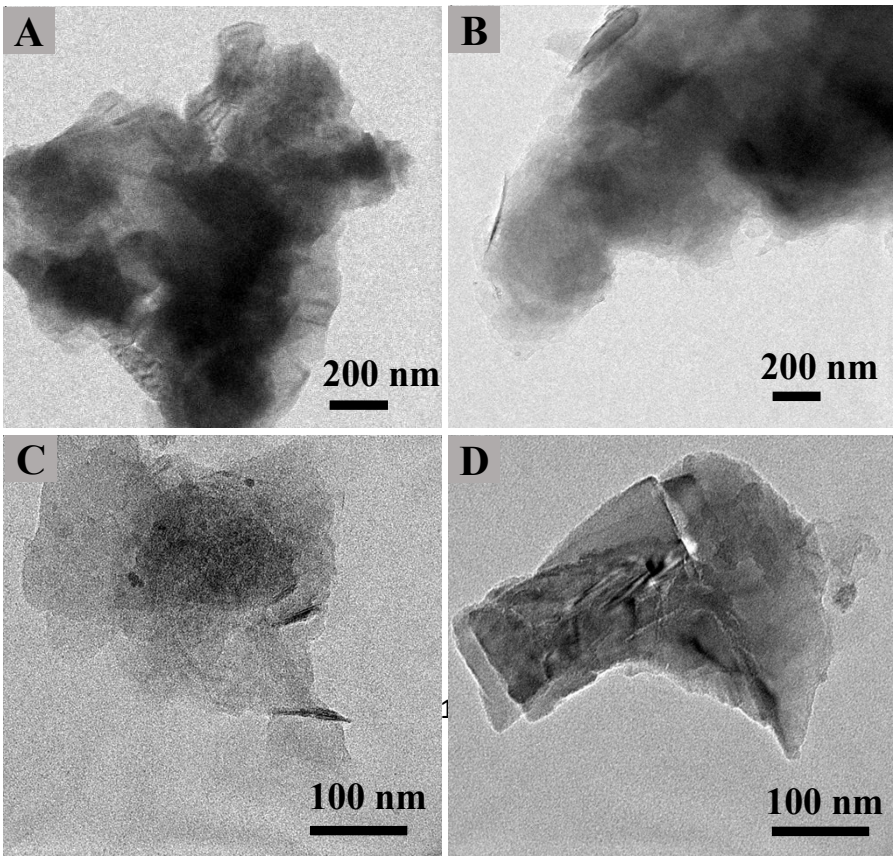

Fig. S4: Nebulization at different gas pressures A) 10 psi, B) 15 psi, C) 20 psi, D) 25 psi.

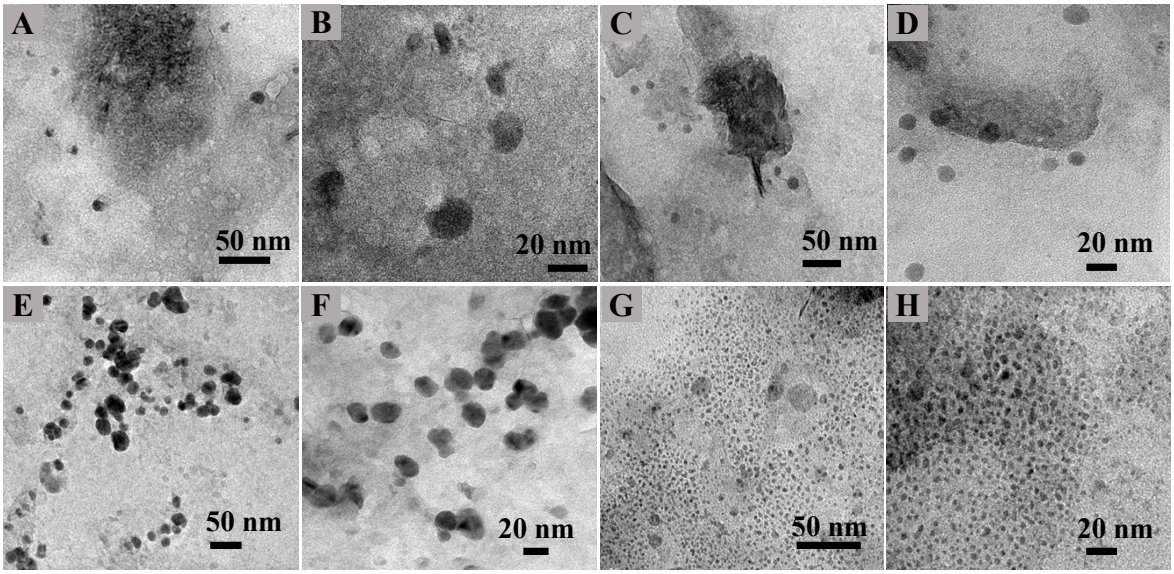

Fig. S5: Effect of applied potential on the electrosprayed MoS_2. A, B) 2.4 kV, C, D) 2.6 kV, E, F) 2.8 kV and G, H) 3.2 kV.

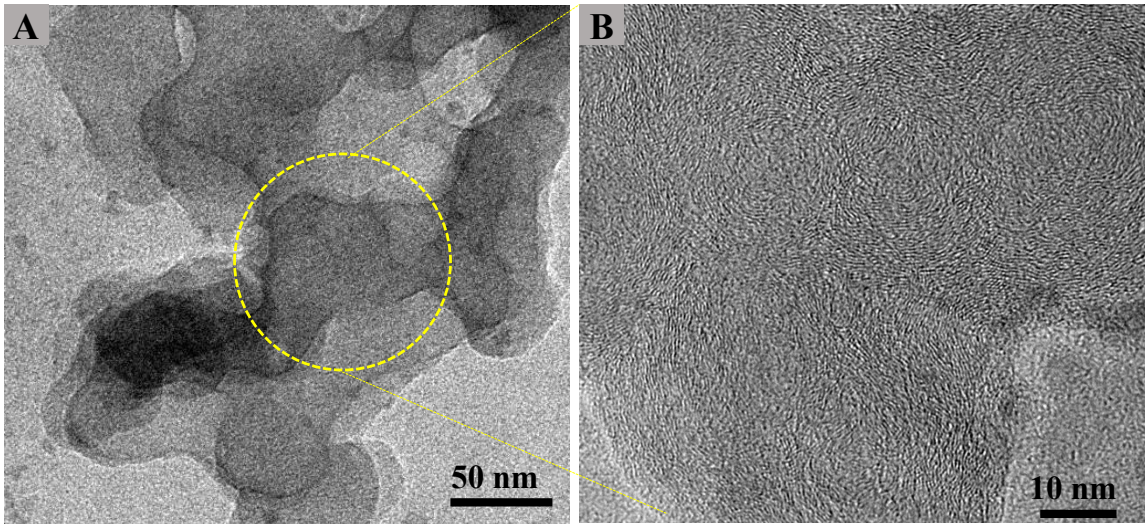

Fig. S6: TEM images showing Inorganic fullerene like (IF) MoS_2 nanoparticles.

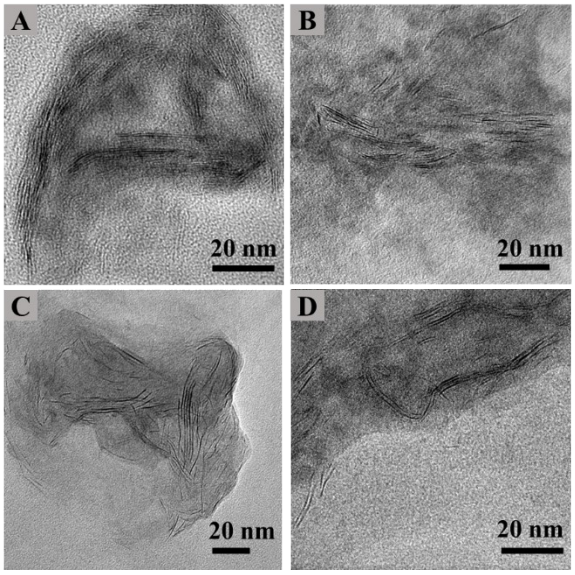

Fig. S7: Effect of solvent on the disintegration process. A) 100% methanol B) 75% methanol C) 50% Methanol D) 25% methanol.

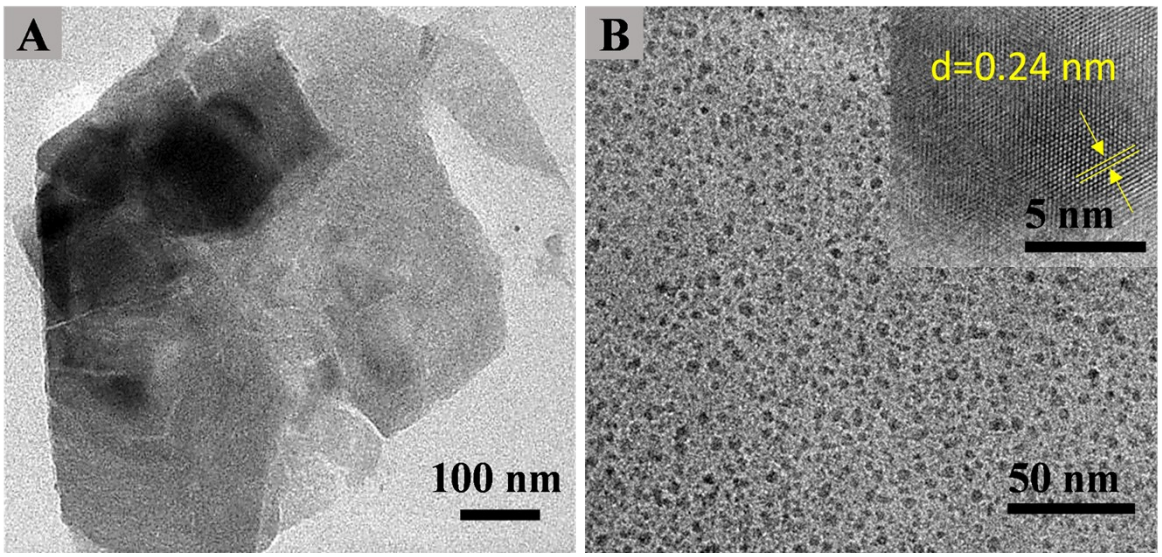
A
100 nm
B
d=0.24 nm
5 nm
50 nm

Fig. S8: Generalization of electrospray process of conversion of 2D materials to 0D materials. A) WS_2 nanosheet before electrospray. B) WS_2 nanoparticles after electrospray. Inset shows the high magnification image of a particle.

References

1 J. K. Lee, K. L. Walker, H. S. Han, J. Kang, F. B. Prinz, R. M. Waymouth, H. G. Nam and R. N. Zare, *Proc. Natl. Acad. Sci. U. S. A.*, 2019, **116**, 19294–19298.

2 S. Banerjee and S. Mazumdar, *Int. J. Anal. Chem.*, 2012, **2012**, 1–40.